

# Components of multifractality in the Central England Temperature anomaly series

Jeferson de Souza,<sup>1,2</sup> Sílvia M. Duarte Queirós,<sup>3</sup> and Alice M. Grimm<sup>4</sup>

<sup>1)</sup>Departamento de Geologia, Universidade Federal do Paraná

PO Box 19027, 81531-980, Curitiba-PR, Brazil

<sup>2)</sup>Centro Estadual de Educação Profissional de Curitiba

Rua Frederico Maurer 3015, 81670-020, Curitiba-PR, Brazil<sup>a)</sup>

<sup>3)</sup>Centro de Física do Porto, Universidade do Porto

Rua do Campo Alegre 687, 4169-007, Porto, Portugal<sup>b)</sup>

<sup>4)</sup>Departamento de Física, Universidade Federal do Paraná

PO Box 19027, 81531-980, Curitiba-PR, Brazil

We study the multifractal nature of the Central England Temperature (CET) anomaly, a time series that spans more than 200 years. The series is analyzed as a complete data set and considering a sliding window of 11 years. In both cases, we quantify the broadness of the multifractal spectrum as well as its components defined by the deviations from the Gaussian distribution and the influence of the dependence between measurements. The results show that the chief contribution to the multifractal structure comes from the dynamical dependencies, mainly the weak ones, followed by a residual contribution of the deviations from Gaussianity. However, using the sliding window, we verify that the spikes in the non-Gaussian contribution occur at very close dates associated with climate changes determined in previous works by component analysis methods. Moreover, the strong non-Gaussian contribution found in the multifractal measures from the 1960s onwards is in agreement with global results very recently proposed in the literature.

PACS numbers: 05.45.Df; 47.53.+n; 92.70.Gt

Keywords: Multi-fractals; Temperature anomaly; Non-stationarity

## I. INTRODUCTION

After Mandelbrot setting forth the concept of fractal, the interest of the scientific community in systems exhibiting self-similarity<sup>1</sup>, *i.e.*, the property by which a system is (approximately) equal to a part of itself has soared. Since then, fractals have been applied to such diverse fields as physiology and economics with the intention of analyzing the existence of scale-invariant behavior. This property can be characterized by a sole fractal (or Hausdorff) dimension or a spectrum of locally dependent exponents, the so-called multifractal spectrum<sup>2-4</sup>. Considering a given observable  $\mathcal{O}$ , the scale invariance (self-similarity) we have mentioned can be mathematically written as,

$$f(\{\lambda \mathcal{O}^z\}) = \lambda^{\alpha(z)} f(\{\mathcal{O}\}). \quad (1)$$

Time series are generally self-affine, *i.e.*, they have different scaling properties in  $x$  and  $y$  directions. When, and only when, the exponent  $\alpha(z)$  is constant for all  $z$ , the system has single scale invariance behavior.

In the field of meteorology and geophysics, fractality and scale invariance are popular concepts as well. However, the large majority of the surveys over self-similarity

of climate time series have been only devoted to the appraisal of memory effects<sup>5-9</sup> introduced in the form of linear correlations or correlations that can be written in a linear way. The existence of memory is quantified by the power spectrum exponent  $\beta$ , which is related to just one specific value  $\alpha$  (the so-called Hurst exponent) of the whole multifractal spectrum. This single  $\alpha$  is related to the power spectrum exponent  $\beta$  via the Wiener-Khinchin relation and to the fractal dimension,  $D$ , by  $D = 2 - H$ . When  $\alpha(z) \neq \text{constant}$ , it is possible to extend these studies beyond standard memory effects in order to explore and perceive a broader range of statistical and dynamical properties.

In this manuscript, we shed light on the multi-self-similar nature of a paradigmatic meteorological time series: the anomaly of the Central England Temperature (CET), which is the largest instrumental daily data set available on the subject. Our work aims at providing reliable quantitative answers to the following questions: *i)* To what extent does the CET anomaly series evince real multifractality? *ii)* What is the weight of each contributing mechanism to the measured self-invariant signature? *iii)* What is the evolution of those contributions and what are the possible pivotal changes in the nature of the system?

The present manuscript is organized as follows: in Sec. II we provide a thorough description of the data analyzed and the methods we employed; in Sec. III we present our results concerning the proposed questions, and in Sec. IV we discuss the conclusions we have reached from our enquiry.

<sup>a)</sup>E-mail address: jdesouza@ufpr.br

<sup>b)</sup>Present address: Istituto dei Sistemi Complessi - CNR

Via dei Taurini, 19, 00185, Roma, Italy; E-mail address: sdqueiro@gmail.com

## II. DATA AND METHODS

### A. The Central England Temperature time series

The data of the Central England Temperature (CET) is the longest instrumental time series, starting in 1772. Owing to its large span, it can be used to perform comparisons between periods in which greenhouse gases emissions were lower and contemporary times. The CET corresponds to a daily average of measured temperatures at different climate stations close to the triangle defined by the English towns of Bristol, Lancashire and London (see Fig. 1)<sup>10–13</sup>.

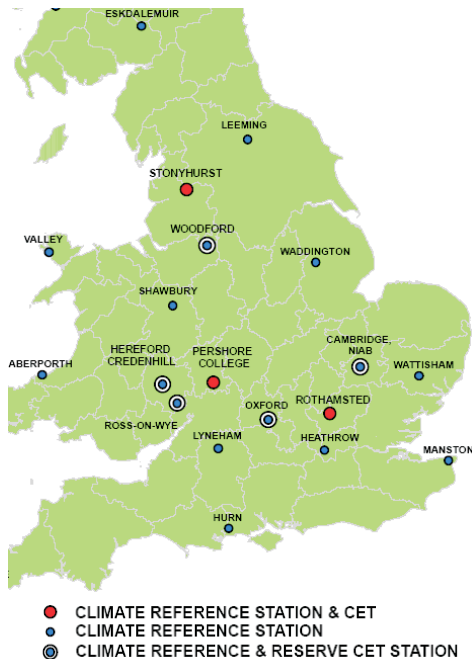


FIG. 1. Excerpt of Great Britain's map with climate stations locations according to the legend shown in the figure. © Crown 2009, the Met Office (Reproduced with permission.)

The first compilation of a monthly series was presented by Manley<sup>10,11</sup> covering the years from 1659 to 1973. Afterwards, these data were updated to 1991 when Parker *et al.* (1992) calculated the daily series. Paying heed to urban warming, the data have been adjusted by 0.1–0.3 Celsius degrees since 1974. From January 1878 until November 2004, the data was recorded by the Met Office using the stations of Rothamsted, Peersshore College and Ringway and from the latter date onwards the station of Stonyhurst replaced Ringway. Concomitantly, revised urban warming and bias adjustments have been applied to the Stonyhurst data. In our work, we specifically set our sights on analyzing the difference between the daily temperature and the average temperature cycle temperature obtained by determining the average over all filed years of the temperature for each day making up a year in the Julian calendar. The data used in this

work have been obtained from KNMI (The Royal Netherlands Meteorological Institute) Climate Explorer website <http://climexp.knmi.nl/> where besides the daily temperature, the temperature anomalies and the seasonal cycles are also provided. The annual average of these time series is presented in Fig. 2.

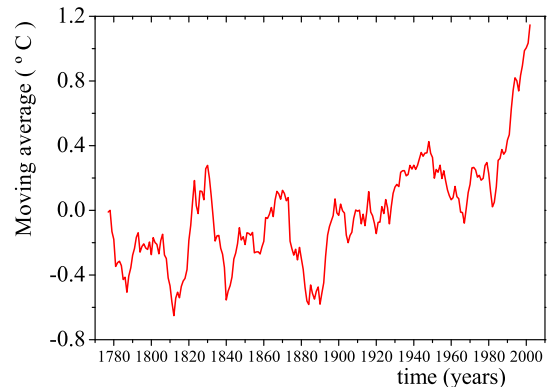


FIG. 2. (Color online) Temperature anomaly (annual average) for the Central England Temperature (CET) time series.

We proceed twofold; First, we analyze the overall self-similar characteristics of the CET anomaly and afterwards we pore over the non-stationarities of the time series. Specifically, we scan the daily time series, from 1772 to 2007, with a 11-year sliding window, in which we apply the same methods that we describe hereinafter. Each window starts on the 1st January of year  $i$  and ends on the 31st December of the year  $i + 10$ , resulting in window of  $11 \times 365$  points. Hence, there will be  $N - 10$  (226) windows whose centers are located at the year  $i + 5$ , where  $N$  is the number of years in the series. We have chosen this sliding window length for the following reasons: *a)* It has approximately  $4k$  data points, which is enough for an accurate estimation of multifractal spectra; *b)* It produces a sufficient number of windows for an appropriate evaluation of the time evolution of scaling properties of the system, since using of larger windows reduce the number of them; *c)* It does not affect our spectra and thus our results, since no spurious scale with frequency of  $1/11\text{years}^{-1}$  was found. In other words, using overlapped instead of simply juxtaposed windows, any significant change that might miss in one windows will be detectable in the next one; *d)* The length of 11 years is large enough to cope with El Niño (La Niña) phenomena.

### B. Methods

#### 1. Multifractal detrended fluctuation analysis - MF-DFA

Detrended fluctuation analysis (DFA) has been pointed out as a tool to monitor climate<sup>14</sup> and such

methodology has been employed in the study of the time evolution of the Hurst exponent of temperature time series, by using of moving windows<sup>15</sup>. Briefly, it corresponds to a method which permits quantifying the way the variance of the cumulative signal scales with the size of the time interval considered for aggregation, after a detrending procedure that seeks to remove non-stationarities of the signal. This method equally weighs large and small deviations and is thus unable to furnish any information on the distinct influence of both cases. Notwithstanding, this method can be easily modified to determine unequal influence of large and small variations or, in other words, to appraise multi-scaling properties: the multifractal detrended fluctuation analysis, MF-DFA.

The MF-DFA<sup>16</sup> is one of the most applied methods to determine the multifractal properties of time series in several fields<sup>17,18</sup>. We have chosen to apply the MF-DFA rather than the Wavelet Transform Modulus Maxima (WTMM)<sup>19</sup> taking into account a recent comparative study in which it has been shown that, in the majority of the situations, the MF-DFA presents reliable results<sup>20</sup>. Specifically, the MF-DFA does not introduce as spurious multifractality as the WTMM.

Considering the time series  $\{x(t)\}$  ( $x$  represents the temperature fluctuation in our case) made up of  $N$  elements, the MF-DFA is composed of the following steps:

- Determine the profile  $Y_i(t)$  that corresponds to the deviation of the signal elements from the mean

$$Y_i(t) = \sum_{l=1}^t [x_i(t) - \langle x \rangle], \quad (1 \leq t \leq N), \quad (2)$$

where  $\langle \dots \rangle$  represents the average over elements and  $i = 1, \dots, N$ .

- Divide the new profile  $Y_i(t)$  into  $N_s \equiv \text{int}(\frac{N}{s})$  non-overlapping intervals of equal size  $s$ ;
- Compute the local trend by a least-squares adjustment method, and thereupon the variance,

$$F^2(\nu, s) = \frac{1}{s} \sum_{l=1}^s \{Y[(\nu-1)s + l] - y_\nu(l)\}^2, \quad (3)$$

for each segment  $\nu = 1, \dots, N_s$ , where  $y_\nu(i)$  represents a  $p^{th}$ -order fitting polynomial in the segment  $\nu$ . Since the number of points in most time series is not a multiple of the number of segments in a given scale  $s$ , the same procedure may be performed on the series with the order of its elements reversed. In this case, the two resulting matrices must be concatenated and the fluctuation function described in the next item must be divided by two. The order of the polynomial is relevant for the results one might obtain. For the CET anomaly time series we used polynomials of  $2^{nd}$ -order.

- Determine the average  $F_z(s)$  over all segments to obtain the fluctuation function of order  $z$ ,

$$F_z(s) \equiv \left\{ \frac{1}{N_s} \sum_{\nu=1}^{N_s} [F^2(\nu, s)]^{z/2} \right\}^{1/z}, \quad \forall z \neq 0, \quad (4)$$

and

$$F_z(s) \equiv \exp \left\{ \frac{1}{2N_s} \sum_{\nu=1}^{N_s} \ln [\tilde{F}^2(\nu, s)] \right\}, \quad z = 0. \quad (5)$$

Equation (4) is basically the only equation different to the DFA method. On the one hand, negative values of  $z$  decrease the influence of large values of  $F^2$ , whereas it augments the influence of small values. On the other hand, positive values of  $z$  have exactly the opposite effect. It is from this outcome that we are able to check the different scales present in the system.

- Assess the scaling behavior of  $F_z(s)$  considering a log-log scale representation of  $F_z(s)$  versus  $s$  for each value of  $z$ . If the series  $\{x(t)\}$  shows multi-scaling features then,

$$F_z(s) \sim s^{h(z)}. \quad (6)$$

When the exponent  $h(z)$  is negative, as in the case of anti-correlated signals, or close to zero, the double summation

$$\tilde{Y}_i(t) = \sum_{l=1}^t [Y_i(t) - \langle Y_i \rangle]; \quad (7)$$

must be used in Eq. (3) in lieu of Eq. (2). This additional step is necessary because the methodology as it was presented is inaccurate for negative generalized Hurst exponents. The generalized fluctuation function (Eq. 6) becomes then

$$\tilde{F}_z(s) \sim s^{\tilde{h}(z)}. \quad (8)$$

where  $\tilde{h}(z) = h(z) + 1$ .

Small fluctuations are generally characterized by large scale values of the exponent  $h(z)$  (and  $z < 0$ ), whereas large fluctuations are typified by small values of  $h(z)$  (and  $z > 0$ ).

Bridging this procedure and the standard formalism, we verify that  $[F_z(s)]^z$  can be interpreted as the partition function,  $Z_z(s)$ ,<sup>21</sup> which is known to scale with the size of the interval as,

$$Z_z(s) \sim s^{\tau(z)}. \quad (9)$$

Hence, according to Eq. (6) and Eq. (9) we have,

$$\tau(z) = z h(z) - 1. \quad (10)$$

Legendre transforming,

$$f(\alpha) = z\alpha - \tau(z), \quad (11)$$

we can relate the exponent  $\tau(z)$  with the exponent,  $\alpha$ ,

$$\alpha = h(z) + z \frac{dh(z)}{dz}, \quad (12)$$

and

$$f(\alpha) = z[\alpha - h(z)] + 1. \quad (13)$$

For  $z = 2$ ,  $h(2) \equiv H$  corresponds to the Hurst exponent customarily determined by methods like the original  $R/S$  ratio or the DFA<sup>22,23</sup> with  $H = (\beta + 1)/2$  and  $\beta$  is the power spectrum exponent according to the Wiener-Khinchin relation. On the other hand,  $z = 0$  give us the support dimension of the self-affine structure. In the case of a monofractal,  $h(z)$  is independent of  $z$  implying homogeneity in the scaling behavior and thus Eq. (10) reduces to  $\tau(z) = zH - 1$ . Explicitly, there exist only different values of  $h(z)$  if large and small fluctuations scale in differently. Lastly, we must stress out we are using the term fractal in not totally formal way. In fact, despite the fact that in some cases  $h(z)$  to the box-counting dimension, it generally does not verify all of the properties to be classified as the Hausdorff-Besicovitch dimension of the signal.

## 2. Components of multifractality

There are two ingredients that induce multifractality in a time series: the deviations from a scale dependent distribution and the dependence between its elements<sup>16</sup>. These factors are generally assumed as independent and thence the total multifractality usually stems from the superposition of both. This means we can accredit a certain value  $h_{\text{NG}}(z)$  to the non-Gaussianity and a value  $h(z) - h_{\text{NG}}(z)$  to the dependence.<sup>1</sup> However, it should be noted that this is not necessarily true. For instance, in the case of heteroscedastic models such as ARCH-like proposals the two elements of multifractality are strongly dependent<sup>24</sup>. This assertion is based on the fact that the non-Gaussianity of the time series comes about from the existence of dependencies between elements that are linear correlations in the (square) volatility. When these dependencies are set to zero, the outcome is a Gaussian series. Consistently, taking into consideration that the variables are uncorrelated, we verify that the two contributions towards multifractality are one and the same. From Eqs. (10)-(13), we can understand that a plain

way of checking the existence of multifractal features is achieved by computing the difference,  $\Delta\alpha$ , between the minimum and the maximum values of the spectrum  $f(\alpha)$ . If there is a mono-fractal nature we shall have  $\Delta\alpha = 0$ , otherwise we should be able to separate out the contributions of the non-Gaussian deviation,  $\Delta\alpha_{\text{NG}}$ , the non-linear dependencies,  $\Delta\alpha_{\text{NL}}$ , and linear features,  $\Delta\alpha_{\text{LD}}$ , so that

$$\Delta\alpha = \Delta\alpha_{\text{NG}} + \Delta\alpha_{\text{LD}} + \Delta\alpha_{\text{NL}}. \quad (14)$$

It is generally assumed that linearities do not contribute to the multifractal broadness because they are traditionally related to a single scale of dependence. However, previous results on financial data<sup>18,25</sup> have showed that this linear/weak dependencies do modify the MF-DFA spectrum and thus we shall a priori not scrap its contribution. Consider that our time series  $\{x(t)\}$  is associated with a non-Gaussian distribution and that its elements exhibit dependencies at a non-null level. If we perform an appropriate shuffling process, we define a new series related to original one by having the same probability density function, but for which there is no dependency between the elements, because the memory was totally destroyed. As proven in ref. 16, when we analyze the multifractal spectrum of the shuffled surrogate, the curve will depart from the mono-fractal behavior,  $\Delta\alpha = \Delta\alpha_{(\text{shuf})} \neq 0$ , due to the non-Gaussianity of the probability density function and thus,

$$\Delta\alpha_{\text{NG}} = \Delta\alpha_{(\text{shuf})}^{\text{eff}}, \quad (15)$$

where  $\Delta\alpha^{\text{eff}}$  is an effective  $\Delta\alpha$  that will be defined shortly. Alternatively, we can apply a procedure of phase randomization in which we Fourier transform the series in the  $\omega$  domain  $[-\pi, \pi)$  and replace the phases by random values (uniformly distributed) up to the first half of the transformed series (excluding the phases of  $\omega = -\pi, 0$ ). The conjugates of the first half are then used for the remaining terms. Afterwards, we apply the Inverse Fourier transform. The final result is a time series in which the previously existing deviations from the Gaussian distribution are destroyed (see an example in Fig. 3). Nonetheless, we can verify that the power spectrum of the surrogate is the same as the original series. Accordingly, since the power spectrum describes the existing linear-correlations, when we evaluate the multifractality of the new series,  $\Delta\alpha_{(\text{rand})}$ , the only contribution originates from the linearities of the system,

$$\Delta\alpha_{\text{LD}} = \Delta\alpha_{(\text{rand})}^{\text{eff}}. \quad (16)$$

When we analyze the multifractal nature of a time series which has been shuffled and phase randomized (or vice-versa) we are supposed to get  $\Delta\alpha_{(\text{shuf}\&\text{rand})} = 0$ . Nevertheless, the values different from zero (considering the error bars) that are found when we compute  $\Delta\alpha_{(\text{shuf}\&\text{rand})}$  are still important as they can be used to check the effect of the error introduced by the finiteness

---

<sup>1</sup> Throughout the text we employ the term non-Gaussianity somewhat inaccurately to refer to a distribution which does not have a defined scale as the Gaussian presents. Nevertheless, it is a more or less established terminology for the absence of scale.

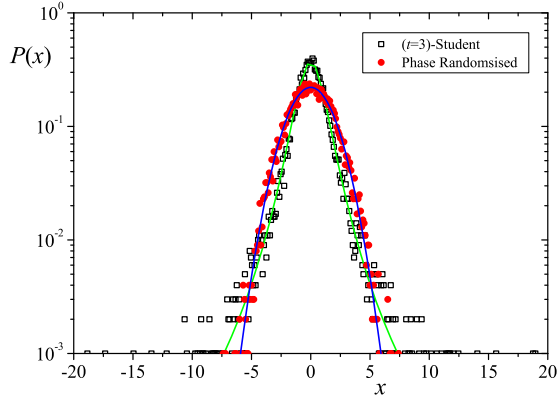


FIG. 3. (Color online) The ( $\square$ ) symbols were obtained from a series of  $10^4$  elements following a ( $t = 3$ )-Student distribution (or a ( $q = 3/2$ )-Gaussian with  $\sigma^2 = 3$ ) which was shuffled in order to remove any possible dependence between the variables due to the pseudo-random generator<sup>26</sup> and the ( $\bullet$ ) symbols were obtained from a surrogate time series originate sprung from the phase randomization procedure which matches a Gaussian distribution with the same standard deviation.

of the time series and the method. This allows us to define the effective  $\Delta\alpha^{\text{eff}}$  as:

$$\Delta\alpha_{(\dots)}^{\text{eff}} = \Delta\alpha_{(\dots)} - \Delta\alpha_{(\text{shuf\&rand})}, \quad (17)$$

for the original, shuffled and random phase time series.

We can make an appraisal of the joint contributions of the non-Gaussianity and the non-linearities as it be-tides ARCH-like processes by proceeding the following way. Instead of randomizing the phases of the Fourier Transform  $\tilde{x}(\omega)$ , we preserve them and assign a constant value to the absolute value of  $\tilde{x}(\omega)$  heading that  $|\tilde{x}(\omega)| = |\tilde{x}(-\omega)|$ . With this, we are setting a constant power spectrum typical of a white noise while preserving every other feature of the dynamics (by preserving the phase). After Inverse Fourier transforming, we can compute the multifractal broadness  $\Delta\alpha_{\text{PP}}$ , the effective value of which is to be compared with the sum of  $\Delta\alpha_{\text{NG}}$  and  $\Delta\alpha_{\text{NL}}$ .

In spite of the fact that the effect of time dependencies in the multifractality is already take into consideration in the MF-DFA procedure (The D stands for *detrended*), it is worth mentioning that in order to apply the Wiener-Khinchin relation the series must be stationary or at least close to it. With the purpose to overcome the problem of the non-stationarity of the time series for a proper evaluation of  $S(\omega)$ , which is only necessary to generate the surrogate series, we have applied a high-pass filter<sup>27</sup> which removes the non-stationarities. We have also used the Burg algorithm<sup>28,29</sup> for estimating  $S(\omega)$  since it is very difficult to distinguish noise from information from the standard FFT spectrum.

### III. RESULTS

#### A. Overall results

In this sub-section we first analyze the time series as a whole set. The results of the multifractal analysis of the CET anomaly time series and its various surrogates described in the previous section are depicted in Fig. 4. For all the curves we verify the fat-fractal nature of the series as the maximum value of  $f(\alpha)$  is equal to 1. By extrapolating the values  $\alpha_{\text{min}}$  and  $\alpha_{\text{max}}$  at which the  $f(\alpha)$  curve intersects the  $\alpha$  axis, we determined the values of  $\Delta\alpha = 0.37$  for the original times series and for the shuffled plus randomized surrogate the multifractal broadness  $\Delta\alpha_{(\text{shuf\&rand})} = 0.16$  yielding an effective broadness  $\Delta\alpha^{\text{eff}} = 0.21$ . Concerning the remaining surrogates we have obtained effective values  $\Delta\alpha_{(\text{shuf})}^{\text{eff}} = \Delta\alpha_{\text{NG}} = 0.02$ ,  $\Delta\alpha_{(\text{rand})}^{\text{eff}} = \Delta\alpha_{\text{LD}} = 0.13$  and  $\Delta\alpha_{\text{NL}} = 0.06$ . Examining the multifractal results of the phase-preserved surrogate we obtained  $\Delta\alpha_{(\text{white})} = 0.05$ . Taking into account the error ( $\pm 0.01$  in our analyses) we verify that  $\Delta\alpha_{\text{PP}} \simeq \Delta\alpha_{\text{NL}} + \Delta\alpha_{\text{NG}}$ .

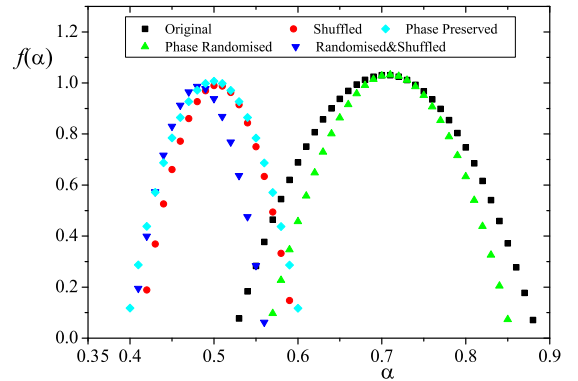


FIG. 4. (Color online) Multifractal spectrum  $f(\alpha)$  vs  $\alpha$  for the original CET anomaly and for the surrogates generated by shuffling, phase randomizing, shuffling plus phase randomizing and phase preservation described in Sec. II B 2 .

The slender contribution of the Non-Gaussianity is easily understandable by the well-known nearness to the Gaussian distribution of the CET anomaly.

These results, particularly the influence of the linear correlations can be double-checked the other way round. Specifically, we can create a new surrogate which retains the power spectrum  $S(\omega)$  (shown in Fig. 5) of the CET anomaly but whose elements are associated with a Normal distribution and which do not present any non-linear dependencies. This can be made by generating a Normal distributed and independent time series that is ultimately Fourier transformed. The amplitude of each element of the set  $\{\tilde{x}(\omega)\}$  is changed by multiplying it by

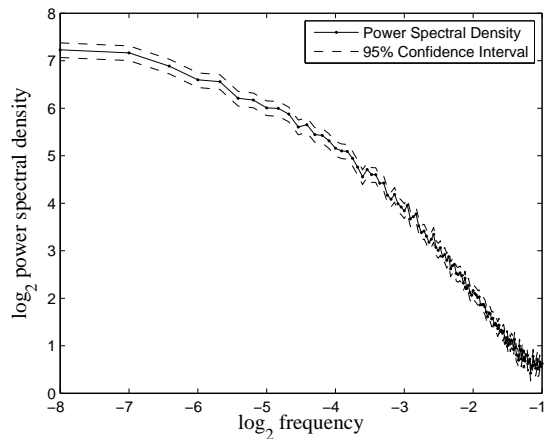


FIG. 5. (Color online) Power spectrum  $S(\omega)$  vs  $\omega$  for the CET anomaly obtained using the Burg algorithm.<sup>28,29</sup> The dashed lines represent the error margins ( 5 % of the power spectrum value).

$\sqrt{S(\omega)}$ . Thereafter, we apply the inverse Fourier transform on this series. The results of this procedure are depicted in Fig. 6, which shows an effective broadness  $\Delta\alpha_{(\text{fourier})}^{\text{eff}} = 0.15$ , completely compatible with the result  $\Delta\alpha_{\text{LD}}$  hereinabove mentioned.

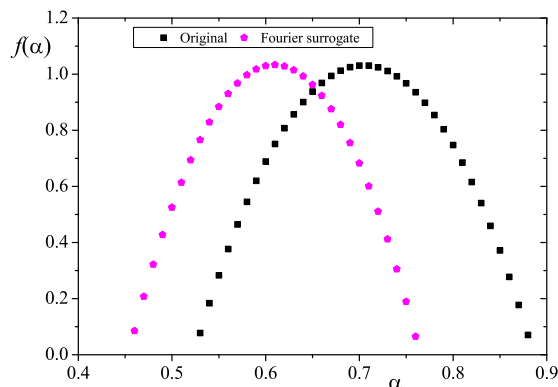


FIG. 6. (Color online) Multifractal spectrum  $f(\alpha)$  vs  $\alpha$  for the original CET anomaly and for the surrogates in which the power spectrum is kept. It is visible that the broadness of both spectra are not far away. Moreover the broadness  $\Delta\alpha_{(\text{Fourier})}$  falls within  $\Delta\alpha_{(\text{rand})}$ .

## B. Time dependence of the components of multifractality

Applying the methods described in the previous section on the CET anomaly time series we identified several

features in the series. The first of all indicates the non-stationary nature of the multifractal spectrum in the time series as depicted in Fig. 7. This multifractal evolution can be tweaked in order to obtain the effective multifractal broadness  $\Delta\alpha^{\text{eff}}$ . The results of this tuning are striking. In average we verified that the effective multifractality represents just about 50% of the broadness obtained in direct measurements of the CET anomaly time series in Fig. 7. Concerning the truthful elements of multifractality we can use Eq. (15) and Eq. (16). For the contribution of the non-Gaussianity,  $\Delta\alpha_{NG}$ , we understood that only 33 out of the 226  $\Delta\alpha_{(\text{shuf})}^{\text{eff}}$  are actually different to zero and consequently to a single-structure nature. This corresponds to an average contribution of merely 3% which once again is in accordance with the almost Gaussian nature of the time series. Regarding the contribution  $\Delta\alpha_{LD}$ , it is obtained when we convert our series into a Gaussian series by means of the phase randomization procedure as we depict in Fig. 8. The average contribution towards the multifractal nature is 59%. Summing the two contributions we grasp that there are missing elements. This implies that the multifractality introduced by the non-linearities corresponds to an average of 38%, as shown in Fig. 9.

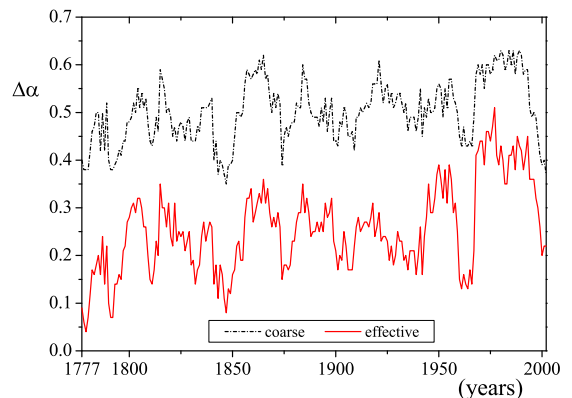


FIG. 7. (Color online) Multifractal broadness  $\Delta\alpha$  of the Central England temperature anomaly between 1777 and 2002, coarse and effective. The  $\Delta\alpha^{\text{eff}}$  is obtained after removing finite size effects and systematic algorithmic error, by subtracting from the original  $\Delta\alpha$ , the value of  $\Delta\alpha_{(\text{shuf}\&\text{rand})}$  as described in Eq. (17). Each curve follows the legend in the figure.

## C. Detecting changes in climate

The results we have presented in the previous subsection can be interestingly compared with the results by Berkes *et al.*<sup>30</sup>. Based on Functional Data Analysis (FDA), Berkes *et al.* pointed out a set of climate

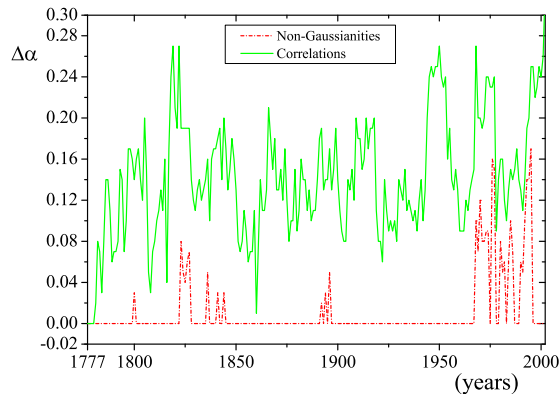


FIG. 8. (Color online) Non-Gaussian and linear dependence (correlations) contributions to the effective multifractal broadness  $\Delta\alpha^{\text{eff}}$  of the Central England temperature anomaly between 1777 and 2002. Each curve follows the legend in the figure. The Non-Gaussian character is related to the broadness of the multifractal spectrum of the shuffled time series, while the linear dependence is related to the broadness of the multifractal spectrum of the randomized time series. All the calculations have been performed using the effective  $\Delta\alpha$  given by Eq. (17).

changes whose major statistical significance occurred in 1780, 1815, 1926 and 2007 for a previous method called MDA and 1780, 1808, 1850, 1926, 1992 and 2007 for their new methodology. Looking to our results we can verify changes in the non-Gaussianity around 1800 followed by flurried periods between 1820-1829, 1834-1845, 1891-1897 and a last and standing ruffled period from 1966 on. Despite each study surveys different quantities, it is well-established that changes in a certain dynamics can be identified from variations in different observables that are associated with that dynamics. It is thus reliable that this fair concurrence provides us with an indication about the robustness of past changes in the leading dynamical mechanism of the temperature. Although we could not observe any change in 1926 or thereabouts in Fig. 8 we noticed that there is a sharp peak close to this date in Fig. 9. It is worthy to be emphasized that the authors of the FDA work refer to the method as a "mere modeling assumption that is useful in identifying patterns of change in mean temperature curves". The broadest and highest contributions of non-linear dependence and non-Gaussianity start from the mid 1960s to the late 1990s. A particular pattern composed of successive positive values in the annual average of the temperature anomaly is reported by Parker *et al.* (1992) in this period, which encloses the change of phase that is well-documented in the climatological temperature<sup>31</sup>. Moreover, we have observed that the spikes verified in the  $\Delta\alpha_{\text{NG}}$  concur with the emergence of kurtosis excess when statistical moments are surveyed<sup>32</sup>. Recent results

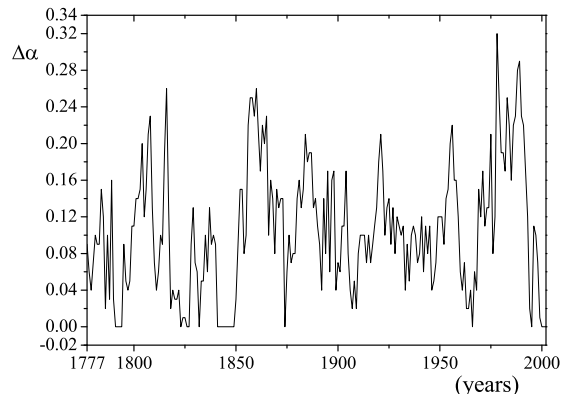


FIG. 9. (Color online) Non-linear dependence contribution to the effective multifractal broadness  $\Delta\alpha^{\text{eff}}$  of the Central England temperature anomaly between 1777 and 2002. The weight of the non-linear dependence contribution are measure from the broadness of the  $f(\alpha)$  curve of the surrogate time series with the same Fourier spectrum of the original one, but without linear correlations. All the calculations have been performed using the effective  $\Delta\alpha$  given by Eq. (17).

published by Hansen *et al.*<sup>33</sup> using a standard statistical approach on a global scale study has verified that the temperature anomaly in the last decades are compatible with non-Gaussian distributions. Motivated out by the time dependence of the scaling properties of the CET anomaly we have made an analysis of the  $\alpha_{\text{min}}$  and  $\alpha_{\text{max}}$  (effective values) that we present in Fig. 10. We took note of the maxima in the amplitude of both spectra that conform with decadal oscillations. Namely, we have found for  $\alpha_{\text{min}}$  maxima at  $16^{-1}$  and  $32^{-1} \text{ year}^{-1}$  and for  $\alpha_{\text{max}}$  maxima at  $17^{-1}$ ,  $34^{-1} \text{ year}^{-1}$  with the former having an extra peak at  $55^{-1} \text{ year}^{-1}$ . These decadal oscillations are not present when the broadness  $\Delta\alpha$  is analyzed. One reason for this stems from the fact that both  $\alpha_{\text{max}}$  and  $\alpha_{\text{min}}$  show very close peaks in the spectrum and thus when the difference between them is considered those peaks are not perceived as we have two co-evolving quantities.

#### IV. FINAL REMARKS AND OUTLOOK

In this manuscript we studied the multifractal features of the CET anomaly. This was carried out by considering the whole time series and by assuming sliding blocks of 11 years. Our results showed that the main component of the multifractal structure of the time series is due to the linear dependencies in the dynamics, followed by non-linear dependencies and with a residual contribution of the deviations to the Gaussianity. Nonetheless, when we analyzed the evolution of multifractality, we verified that until 1950 the non-Gaussian contribution comes



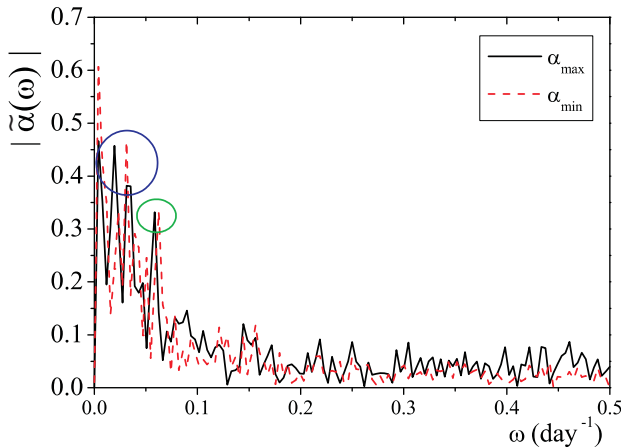


FIG. 10. (Color online) Amplitude of Fourier transform ( $\tilde{\alpha}(\omega)$ ) of the maximum and the minimum values of  $\alpha(t)$ , against frequency. Here  $t$  represents the center of the slide window. The circles identify the local maxima described in the text.

about in periods close to dates at which occurred climate changes according to the results obtained by Functional Data Analysis<sup>30</sup>. From the 1960s onwards the contribution of the non-Gaussianity becomes significant most of the time, a result that matches a recent finding of temperature anomalies significantly beyond the  $3\sigma$  criterion that characterize the validity (or not) of the Gaussian distribution<sup>33</sup>.

Finally, although the scope of the present work concerns the quantitative description of the temperature anomaly multifractality and its ingredients as well as its connection with climatic changes, our analysis can have direct implications in temperature anomaly modeling. Our results point out that the temperature variability modeling must take into account the multifractal nature of the temperature time series, and the contribution of each ingredient for the multifractality, as well. A tentative dynamical scenario is that wherein we resort to the statistical mechanics relation between temperature and standard deviation, *i.e.*, the temperature is proportional to the standard deviation, and consider a model inspired in cascade models of the latter quantity for turbulent fluids such as those introduced in refs. 34–36. Instead of considering a cascade processes in the standard deviation of the quantity upon analysis, we reinterpret those models considering a cascade processes for the average value of the observable, which in this case is the temperature anomaly, so that the average value over a certain scale  $\ell$  comes from the multiplicative process,

$$\mu_\ell(t) = \prod_{i=0}^{n-1} f(i \rightarrow i+1) \mu_L, \quad (18)$$

with  $\mu_L$  representing the average over a reference period  $L$ , *e.g.*  $L = 11$  years, and  $f$  representing the fraction of measure (average) passing from a earlier generation

(time scale) to the subsequent. For this case the greater  $i$ , the smaller  $\ell$ , *i.e.*,  $i = 0$  corresponds to  $\ell = L$  and  $\ell = n$  yields the scale of the temperature anomaly we are willing to describe. Accordingly, the temperature anomaly,  $\xi$ , would be equal to,

$$\xi_\ell(t) = \varepsilon(t) + \mu_\ell(t), \quad (19)$$

where  $\varepsilon$  represents a Gaussian independent and identically distributed noise with zero average and appropriate standard deviation. A skew distribution of  $\mu_L$  will lead to a skew distribution of  $\xi$  as well. Concomitantly, in order to represent the slight kurtosis we can consider a further contribution,  $\zeta$ , coming from a multiplicative noise process,

$$\zeta(t) = \eta(t) \sigma(t) h(t), \quad (20)$$

with  $\sigma(t)$  being a function of past values of  $\xi$  and  $\zeta$  in a heteroscedastic way (see for details 37 and 38) and  $\eta$  another Gaussian noise not correlated with  $\varepsilon$ . The  $\zeta$  contribution is modulated by a step function  $h(t) = \Theta[t - (\Upsilon - \Delta\Upsilon)] \Theta[\Upsilon + \Delta\Upsilon - t]$  where the center of the intervals come from a shot noise following a frequency related to Fig. 10. Mathematically, the probability of having a contribution from  $\zeta$  arising from a perturbation centered at time  $\Upsilon$  is given by,

$$p(\Upsilon) \propto \sum_i \delta(\Upsilon - \Upsilon_i), \quad (21)$$

and the total temperature anomaly will thus correspond to the sum of  $\xi_\ell(t)$  and  $\zeta(t)$ .

Alternative models can be presented, namely the mimicking of the fluctuations of the temperature anomaly instead of that quantity. However, it is simple to find one quantity after the other bearing in mind their relation and statistical properties as in happens in other problems such as fluid turbulence and price dynamics in financial markets. To conclude, we would like to mention that the mechanisms for the definition of surrogates that we described, namely the phase preservation, can be useful in the enquiry into the Gaussian nature of the primary noise in processes as those introduced in previously published work.

## 1. Acknowledgements

We would like to thank the Met Office for kindly providing us with the map in Fig. 1. AMG has received funding from CNPq (Brazilian National Council for Scientific and Technological Development), and from the EU Seventh Framework Programme (FP7/2007-2013) under Grant Agreement nr 212492 (CLARIS LPB. A Europe-South America Network for Climate Change Assessment and Impact Studies in La Plata Basin). JdS acknowledges CNPq, PETROBRAS/FUNPAR-UFPR, Setor de Ciências Exatas - UFPR and Setor de Ciências da Terra - UFPR for support and S. H. S. Schwab, F. Mancini,



F. J. F. Ferreira, are also thanked for valuable helping and encouragement. SMDQ thanks the LABAP laboratory of Universidade Federal do Paraná for the warm hospitality during his visits to the institution sponsored by CNPq and PETROBRAS/FUNPAR-UFPR and the European Commission through the Marie Curie Actions FP7-PEOPLE-2009-IEF (contract nr 250589) in the final part of this work.

- <sup>1</sup>B. B Mandelbrot, *The Fractal Geometry of Nature*. W. H. Freeman and Co., New York (1982).
- <sup>2</sup>Mandelbrot BB (1999) *Multifractals and 1/f Noise*. Springer, New York.
- <sup>3</sup>Schertzer D. and Lovejoy S. (eds.) (1991) *Scaling, Fractals and Non-Linear Variability in Geophysics*. Kluwer, Boston.
- <sup>4</sup>Falconer K (1990) *Fractal Geometry: Mathematical Foundations and Applications*. Wiley, New York.
- <sup>5</sup>Dyer TGJ (1976) An analysis of Manley's central England temperature data: I. Q.J.R. Meteorol. Soc. 102(434), 871888.
- <sup>6</sup>Bain WC (1976) The power spectrum of temperatures in central England. Q.J.R. Meteorol. Soc. 102(432), 464466.
- <sup>7</sup>Lovejoy S and Schertzer D (1986) Scale invariance in climatological temperatures and the spectral plateau. *Annales Geophys.* 4B, 401-410.
- <sup>8</sup>Matyasovszky I (1989) Further results of the analysis of central England temperature data. *Theoretical and Applied Climatology*. 39(3), 126-136
- <sup>9</sup>Pelletier JD (1998) The power spectral density of atmospheric temperature from time scales of 10 to 10<sup>6</sup> yr. *Earth and Planetary Science Letters*. 158 157164
- <sup>10</sup>Manley G (1953) The mean temperature of central England, 1698-1952. *Quarterly Journal of the Royal Meteorological Society* 79(340):242-261.
- <sup>11</sup>Manley G (1974) Central England temperatures: monthly means 1659 to 1973. *Quarterly Journal of the Royal Meteorological Society* 100(425): 389-405.
- <sup>12</sup>Parker DE, Legg TP, Folland CK (1992) A new daily Central England Temperature series 1772-1991. *Int. J. Clim.* 12:317.
- <sup>13</sup>D.E. Parker, E. B. Horton (2005) Uncertainties in central England temperature 1878-2003 and some improvements to the maximum and minimum series. *Int. J. Climatology* 25:1173-1188.
- <sup>14</sup>Kurnaz ML (2004) Detrended fluctuation analysis as a statistical tool to monitor the climate. *J. Stat. Mech.* P07009
- <sup>15</sup>Alvarez-Ramirez J, Alvarez J, Dagdug L, Rodriguez E, Carlos Echeverria J (2008) Long-term memory dynamics of continental and oceanic monthly temperatures in the recent 125 years. *Physica A: Statistical Mechanics and its Applications* 387(14):3629-3640.
- <sup>16</sup>Kantelhardt JW, Zschiegner SA, Koscielny-Bunde E, Havlin S, Bunde A, and Stanley HE (2002) Multifractal detrended fluctuation analysis of nonstationary times series. *Physica A* 316:87-114.
- <sup>17</sup>Ivanov PCh, Amaral LAN, Goldberger AL, Havlin S, Rosenblum MG, Stanley HG, Struzik ZR (1991) From 1/f noise to multifractal cascades in heartbeat dynamics. *Chaos* 11:641-652.
- Matia K, Ashkenazy Y, Stanley HE (2003) Multifractal properties of price fluctuations of stocks and commodities. *Europhys Lett* 61:422-428.
- Ashkenazy Y, Baker DR, Gildor H, Havlin S. (2003) Nonlinearity and multifractality of climate change in the past 420,000 years. *Geophys Res Lett* 30:2146.
- Telesca L, Lapenna V, Macchiato M (2005) Multifractal fluctuations in earthquake-related geoelectrical signals. *New J Phys* 7:214.
- Duarte Queirós SM, Moyano LG, de Souza S, Tsallis C (2007) A nonextensive approach to the dynamics of financial observables. *Eur Phys JB* 55:161-167.
- Niu M-R, Zhou W-X, Yan Z-Y, Guo Q-H, Liang Q-F, Wang F-C, Yu Z-H (2008) Multifractal detrended fluctuation analysis of combustion flames in four-burner impinging entrained-flow gasifier. *Chem Eng J* 143:230.
- <sup>18</sup>Zhou W-X (2009) The components of empirical multifractality in financial returns. *EPL* 88:28004; Zhou W-X (2012) Finite-size effect and the components of multifractality in financial volatility. *Chaos, Solitons & Fractals* 45:147
- <sup>19</sup>Muzy JF, Bacry E, Arneodo A. (1991) Wavelets and multifractal formalism for singular signals: Application to turbulence data. *Phys. Rev. Lett.* 1991;67:3515-3518.
- <sup>20</sup>Oświęcimka P, Kwapien J, Drożdż S (2006) Wavelet versus detrended fluctuation analysis of multifractal structures. *Phys Rev E* 74:016103.
- <sup>21</sup>Feder J (1988) *Fractals*. Plenum, New York.
- <sup>22</sup>Peng C-K, Buldyrev SV, Havlin S, Simons M, Stanley HE, Goldberger AL (1994) Mosaic organization of DNA nucleotides. *Phys Rev E* 49:1685-1689.
- <sup>23</sup>Hurst HE (1951) Long-term storage capacity of reservoirs. *Trans Am Soc Civ Eng* 116:770-808.
- <sup>24</sup>Gourieroux C and Montfort (1996) *A Statistics and Econometric Models*. Cambridge: Cambridge University Press.
- <sup>25</sup>de Souza S and Duarte Queirós SM (2007) Effective multifractal features of high-frequency price fluctuations time series and l-variability diagrams. *Chaos, Solitons & Fractals* 42:2512-2521
- <sup>26</sup>Gentle JE (1995) *Random Number Generation and Monte Carlo Methods*, 2nd ed. Wiley, New York.
- <sup>27</sup>Paarmann LD (2001) *Design and Analysis of Analog Filters - A Signal Processing Perspective*. Kluwer, Dordrecht.
- <sup>28</sup>Marple SL (1987) *Digital Spectral Analysis*. Prentice-Hall, Englewood Cliffs - NJ.
- <sup>29</sup>Stoica P and Moses RL (1997) *Introduction to Spectral Analysis*. Prentice-Hall, Englewood Cliffs - NJ.
- <sup>30</sup>Berkes I, Gabrys R, Horváth L, Kokoszka P (2009) Detecting changes in the mean of functional observations. *Journal of the Royal Statistical Society B* 71:927-946.
- <sup>31</sup>IPCC 2007 Climate Change 2007 - The Physical Science Basis Contribution of Working Group I to the Fourth Assessment Report of the IPCC. <http://www.ipcc.ch>
- <sup>32</sup>de Souza J, Duarte Queirós SM and Grimm AM (2008) Time dependence of the multifractal spectrum and other statistical properties of the Central England Temperature time series. XXXI Encontro Nacional de Física da Matéria Condensada. Águas de Lindóia, Brazil.
- <sup>33</sup>J. Hansen, M. Sato and R. Reudy, *Proc. Nat. Acad. Sci. USA*, DOI:10.1073/pnas.1205276109 (2012)
- <sup>34</sup>Meneveau C and Sreenivasan KR (1987) Simple multifractal cascade model for fully developed turbulence. *Phys. Rev. Lett.* **59**, 1424.
- <sup>35</sup>Castaing B, Gagne Y and Hopfinger EJ (1990) Velocity probability density functions of high Reynolds number turbulence. *Physica D* **46** 177.
- <sup>36</sup>Arneodo A, Muzy JF and Roux SG (1997) Experimental analysis of self-similarity and random cascade processes: application to fully developed turbulence data. *J. Phys. II France* **7** 363.
- <sup>37</sup>Queirós SMD and Tsallis C (2005) On the connection between financial processes with stochastic volatility and nonextensive statistical mechanics. *Eur. Phys. J. B* **S49** 139.
- <sup>38</sup>Andersen TG, Bollerslev T, Diebold FX (2010) Parametric and nonparametric volatility measurement. In: Aït-Sahalia Y, ed. *Handbook of Financial Econometrics*, volume 1, tools and techniques. Elsevier, Amsterdam.